

Perturbative QCD predictions for the small x behaviour of unpolarized and polarized deep inelastic scattering structure functions ¹

J. Kwieciński

Department of Physics

University of Durham

Durham, UK

and

Department of Theoretical Physics

H. Niewodniczański Institute of Nuclear Physics

Kraków, Poland. ²

Abstract

The perturbative QCD predictions for the small x behaviour of the nucleon structure functions $F_{2,L}(x, Q^2)$ and $g_1(x, Q^2)$ are summarized. The importance of the double logarithmic terms for the small x behaviour of the spin structure function $g_1(x, Q^2)$ is emphasised. These terms correspond to the contributions containing the leading powers of $\alpha_s \ln(1/x)^2$ at each order of the perturbative expansion. In the non-singlet case they can be approximately accounted for by the ladder diagrams with quark (antiquark) exchange. We solve the corresponding integral equation with the running coupling effects taken into account and present estimate of the effective slope controlling the small x behaviour of the non-singlet spin structure function $g_1(x, Q^2)$ of a nucleon.

¹ to appear in special issue of Acta Physica Polonica
in honour of Professor Wojciech Królikowski's 70th birthday

²Permanent address

1. Introduction

Analysis of the deep inelastic scattering structure functions in the limit of small values of the Bjorken parameter x allows to test perturbative QCD in a new and hitherto unexplored regime [1, 2, 3]. The advent of the HERA ep collider has opened up an experimental possibility to confront the theoretical QCD expectations with the experimental data on deep inelastic scattering in the small x region. The relevant theoretical framework is provided in this case by the Balitzkij, Fadin, Kuraev, Lipatov (BFKL) equation for the unintegrated gluon distribution $f(x, Q_t^2)$, where Q_t denotes the transverse momentum of the gluon and x its longitudinal momentum fraction [4]. This equation sums the leading powers of $\ln(1/x)$ at each order of the perturbative expansion i.e. it corresponds to the leading $\ln(1/x)$ approximation. The small x behaviour of the structure functions is driven by the gluon through the $g \rightarrow q\bar{q}$ transitions [5].

Perturbative QCD predicts a strong increase of structure functions with the decreasing parameter x and the experimental data from HERA are consistent with this prediction [6, 7]. This increase is much stronger than that which would follow from the expectations based on the "soft" pomeron exchange mechanism with the soft pomeron intercept $\alpha_{soft} \approx 1.08$ as determined from the phenomenological analysis of total hadronic and real photoproduction cross-sections [8].

The small x behaviour of structure functions for fixed Q^2 reflects the high energy behaviour of the virtual Compton scattering total cross-section with increasing total CM energy squared W^2 since $W^2 = Q^2(1/x - 1)$. The Regge pole exchange picture [9] is therefore quite appropriate for the theoretical description of this behaviour. The high energy behaviour which follows from perturbative QCD is often referred to as being related to the "hard" pomeron in contrast to the soft pomeron describing the high energy behaviour of hadronic and photoproduction cross-sections.

The pomeron does not contribute to the spin dependent structure function $g_1(x, Q^2)$ which is controlled by the exchange of reggeons corresponding to axial vector mesons [10]. The pomeron also decouples, of course, from the "non-singlet" part of the unpolarized structure functions i.e. from the combination $F_2^p - F_2^n$ which at small x is controlled by the A_2 reggeon exchange. The small x behaviour of the structure function $g_1(x, Q^2)$ in perturbative QCD is sensitive to a new class of double logarithmic $\ln(1/x)$ contributions i.e. to the terms which contain powers of $\alpha_s \ln^2(1/x)$ in the perturbative expansion [11, 12, 13, 14, 15]. These terms invalidate naive Regge pole model expectations and generate the singular small x behaviour of the structure function $g_1(x, Q^2)$.

The purpose of this paper is to briefly summarize some of the QCD expectations concerning the small x behaviour of the unpolarized and polarized structure functions of the nucleon. In the next section we recall the Regge pole model expectations for the small x behaviour of both the polarized and unpolarized structure functions while section 3 is devoted to the discussion of the BFKL equation [4] and its generalization based on angular ordering, i.e. the Catani, Ciafaloni, Fiorani and Marchesini (CCFM) equation [16, 17, 18]. In Sec. 4 we discuss the small x behaviour of the polarized structure function $g_1(x, Q^2)$ concentrating for simplicity on its non-singlet part. We recall the (approximate) integral equation which resums the double logarithmic terms and discuss its solution after taking into account the running coupling effects. We present an estimate of the effec-

tive slope λ controlling the small x behaviour of the spin-dependent structure function $g_1^{NS}(x, Q^2) = g_1^p(x, Q^2) - g_1^n(x, Q^2) \sim x^{-\lambda}$. Sec. 5 will contain our main conclusions.

2. Regge pole model expectations for the small x behaviour of structure functions

The Regge pole model describes the high energy behaviour of scattering amplitudes in terms of the exchange of reggeons which correspond to poles in the complex angular momentum plane in the crossed channel [9]. The total cross-sections are related through the optical theorem to the imaginary part of the scattering amplitudes in forward direction (i.e. for $t = 0$ where t denotes the momentum transfer squared). The Regge pole model description of the scattering amplitudes when combined with the optical theorem gives therefore automatically predictions for the high energy behaviour of the total cross-sections:

$$\sigma_{ab}^{tot}(s) \sim \frac{1}{s} \text{Im} A_{ab;ab}(s, t=0) = \sum_i \beta_i \left(\frac{s}{s_0} \right)^{\alpha_i(0)-1}. \quad (1)$$

The quantities $\alpha_i(0)$ are the intercepts of the Regge trajectories and β_i denote the couplings.

The Regge pole exchange is to a large extent a generalization of the single particle exchange and so the reggeons carry the same quantum numbers as hadrons which particular Regge pole trajectories correspond to. There is an obvious hierarchy of Regge pole contributions depending upon the magnitude of their intercept. The contribution with highest intercept corresponds to pomeron which carries vacuum quantum numbers.

The high energy behaviour of the total hadronic and (real) photoproduction cross-sections can be economically described by two contributions: an (effective) pomeron with its intercept slightly above unity (~ 1.08) and the leading meson Regge trajectories with intercept $\alpha_R(0) \approx 0.5$ [8]. The reggeons can be identified as corresponding to ρ, ω, f or A_2 exchange(s) depending upon the quantum numbers involved. All these reggeons have approximately the same intercept. One refers to the pomeron obtained from the phenomenological analysis of hadronic total cross sections as the "soft" pomeron since the bulk of the processes building-up the cross sections are low p_t (soft) processes.

The Regge pole model gives the following parametrization of the deep inelastic scattering structure function $F_2(x, Q^2)$ at small x

$$F_2(x, Q^2) = \sum_i \tilde{\beta}_i(Q^2) x^{1-\alpha_i(0)}. \quad (2)$$

The relevant reggeons are those which can couple to two (virtual) photons. The (singlet) part of the structure function F_2 is controlled at small x by pomeron exchange, while the non-singlet part $F_2^{NS} = F_2^p - F_2^n$ by A_2 reggeon. Neither pomeron nor A_2 reggeons couple to the spin structure function $g_1(x, Q^2)$ which is described at small x by the exchange of reggeons corresponding to axial vector mesons [10] i.e. to A_1 exchange for the non-singlet part $g_1^{NS} = g_1^p - g_1^n$ etc.

$$g_1^{NS}(x, Q^2) = \gamma(Q^2) x^{-\alpha_{A_1}(0)} \quad (3)$$

The reggeons which correspond to axial vector mesons are expected to have very low intercept (i.e. $\alpha_{A_1} \leq 0$ etc.)

Several of the Regge pole model expectations for structure functions are modified by perturbative QCD effects as will be briefly described in the forthcoming Sections.

3. BFKL pomeron and QCD predictions for the small x behaviour of the unpolarized structure function

At small values of the parameter x the dominant role is played by the gluons. The basic quantity is an unintegrated gluon distribution $f(x, Q_t^2)$ where x denotes the momentum fraction of a parent hadron carried by a gluon and Q_t its transverse momentum. The unintegrated distribution $f(x, Q_t^2)$ is related in the following way to the more familiar scale dependent gluon distribution $g(x, Q^2)$:

$$xg(x, Q^2) = \int^{Q^2} \frac{dQ_t^2}{Q_t^2} f(x, Q_t^2). \quad (4)$$

In the leading logarithmic approximation the unintegrated distribution $f(x, Q_t^2)$ satisfies the BFKL equation [4] which has the following form:

$$f(x, Q_t^2) = f^0(x, Q_t^2) + \bar{\alpha}_s \int_x^1 \frac{dx'}{x'} \int \frac{d^2q}{\pi q^2} \left[\frac{Q_t^2}{(\mathbf{q} + \mathbf{Q}_t)^2} f(x', (\mathbf{q} + \mathbf{Q}_t)^2) - f(x', Q_t^2) \Theta(Q_t^2 - q^2) \right] \quad (5)$$

where

$$\bar{\alpha}_s = \frac{3\alpha_s}{\pi}. \quad (6)$$

The first and the second terms in the right hand side of eq. (5) correspond to the real gluon emission with q being the transverse momentum of the emitted gluon, and to the virtual corrections respectively. $f^0(x, Q_t^2)$ is a suitably defined inhomogeneous term.

After resumming the virtual corrections and "unresolvable" gluon emissions ($q^2 < \mu^2$) where μ is the resolution defining the "resolvable" radiation, equation (5) can be rearranged into the following "folded" form:

$$f(x, Q_t^2) = \hat{f}^0(x, Q_t^2) + \bar{\alpha}_s \int_x^1 \frac{dx'}{x'} \int \frac{d^2q}{\pi q^2} \Theta(q^2 - \mu^2) \Delta_R\left(\frac{x}{x'}, Q_t^2\right) \frac{Q_t^2}{(\mathbf{q} + \mathbf{Q}_t)^2} f(x', (\mathbf{q} + \mathbf{Q}_t)^2) + O(\mu^2/Q_t^2) \quad (7)$$

where

$$\Delta_R(z, Q_t^2) = z^{\bar{\alpha}_s \ln(Q_t^2/\mu^2)} = \exp\left(-\bar{\alpha}_s \int_z^1 \frac{dz'}{z'} \int_{\mu^2}^{Q_t^2} \frac{dq^2}{q^2}\right) \quad (8)$$

and

$$\hat{f}^0(x, Q_t^2) = \int_x^1 \frac{dx'}{x'} \Delta_R\left(\frac{x}{x'}, Q_t^2\right) \frac{df^0(x', Q_t^2)}{d\ln(1/x')} \quad (9)$$

Equation (7) sums the ladder diagrams with reggeized gluon exchange along the chain with the gluon trajectory $\alpha_G(Q_t^2) = 1 - \frac{\bar{\alpha}_s}{2} \ln(Q_t^2/\mu^2)$.

For the fixed coupling case eq.(5) can be solved analytically and the leading behaviour of its solution at small x is given by the following expression:

$$f(x, Q_t^2) \sim (Q_t^2)^{\frac{1}{2}} \frac{x^{-\lambda_{BFKL}}}{\sqrt{\ln(\frac{1}{x})}} \exp\left(-\frac{\ln^2(Q_t^2/\bar{Q}^2)}{2\lambda'' \ln(1/x)}\right) \quad (10)$$

with

$$\lambda_{BFKL} = 4\ln(2)\bar{\alpha}_s \quad (11)$$

$$\lambda'' = \bar{\alpha}_s 28\zeta(3) \quad (12)$$

where the Riemann zeta function $\zeta(3) \approx 1.202$. The parameter \bar{Q} is of nonperturbative origin.

The quantity $1 + \lambda_{BFKL}$ is equal to the intercept of the so called BFKL pomeron. Its potentially large magnitude (~ 1.5) should be contrasted with the intercept $\alpha_{soft} \approx 1.08$ of the (effective) "soft" pomeron which has been determined from the phenomenological analysis of the high energy behaviour of hadronic and photoproduction total cross-sections [8].

In practice one introduces the running coupling $\bar{\alpha}_s(Q_t^2)$ in the BFKL equation (5). This requires introduction of the infrared cut-off that would prevent entering the infrared region where the coupling becomes large. The effective intercept λ_{BFKL} found by numerically solving the equation depends on the magnitude of this cut-off [19].

The structure functions $F_{2,L}(x, Q^2)$ are described at small x by the diagram of Fig.1 which gives the following relation between the structure functions and the unintegrated distribution f :

$$F_{2,L}(x, Q^2) = \int_x^1 \frac{dx'}{x'} \int \frac{dQ_t^2}{Q_t^2} F_{2,L}^{box}(x', Q_t^2, Q^2) f\left(\frac{x}{x'}, Q_t^2\right). \quad (13)$$

The functions $F_{2,L}^{box}(x', Q_t^2, Q^2)$ may be regarded as the structure functions of the off-shell gluons with virtuality Q_t^2 . They are described by the quark box (and crossed box) diagram contributions to the photon-gluon interaction in the upper part of the diagram of Fig. 1. The small x behaviour of the structure functions reflects the small z ($z = x/x'$) behaviour of the gluon distribution $f(z, Q_t^2)$.

The equation (13) is an example of the " k_t factorization theorem" which relates measurable quantities (like DIS structure functions) to the convolution in both longitudinal as well as in transverse momenta of the universal gluon distribution $f(z, Q_t^2)$ with the cross-section (or structure function) describing the interaction of the "off-shell" gluon with the hard probe [20]. The k_t factorization theorem is a basic tool for calculating observable quantities in the small x region in terms of the (unintegrated) gluon distribution f which is the solution of the BFKL equation.

A more general treatment of the gluon ladder is provided by the CCFM equation based on angular ordering along the gluon chain [17, 18]. This equation embodies both

the BFKL equation at small x and the conventional Altarelli-Parisi evolution at large x . The unintegrated gluon distribution f now acquires dependence upon an additional scale Q which specifies the maximal angle of gluon emission. The CCFM equation has a form analogous to that of the "folded" BFKL equation (7):

$$f(x, Q_t^2, Q^2) = \hat{f}^0(x, Q_t^2, Q^2) + \bar{\alpha}_s \int_x^1 \frac{dx'}{x'} \int \frac{d^2q}{\pi q^2} \Theta(Q - qx/x') \Delta_R\left(\frac{x}{x'}, Q_t^2, q^2\right) \frac{Q_t^2}{(\mathbf{q} + \mathbf{Q}_t)^2} f(x', (\mathbf{q} + \mathbf{Q}_t)^2, q^2) \quad (14)$$

where the theta function $\Theta(Q - qx/x')$ reflects the angular ordering constraint on the emitted gluon. The "non-Sudakov" form-factor $\Delta_R(z, Q_t^2, q^2)$ is now given by the following formula:

$$\Delta_R(z, Q_t^2, q^2) = \exp \left[-\bar{\alpha}_s \int_z^1 \frac{dz'}{z'} \int \frac{dq'^2}{q'^2} \Theta(q'^2 - (qz')^2) \Theta(Q_t^2 - q'^2) \right] \quad (15)$$

Eq.(14) still contains only the singular term of the $g \rightarrow gg$ splitting function at small z yet its generalization which would include the remaining parts of this vertex (as well as quarks) is possible.

In Fig. 2 we show the results for the structure function F_2 calculated from the k_t factorization theorem with the function f obtained from the CCFM equation [21]. We confront these predictions with the most recent data from the H1 and ZEUS collaborations at HERA [6, 7] as well as with the results of the analysis which was based on the Altarelli-Parisi equation alone without the small x resummation effects being included in the formalism [22, 23]. In the latter case the singular small x behaviour of the gluon and sea quark distributions has to be introduced in a parametrization of the starting distributions at the moderately large reference scale $Q^2 = Q_0^2$ (i.e. $Q_0^2 \approx 4\text{GeV}^2$ or so) [22]. One can also generate the singular behaviour dynamically starting from the non-singular "valence-like" parton distributions at some very low scale $\mu_0^2 = 0.35\text{GeV}^2$ [23]. In the latter case the gluon and sea quark distributions exhibit the following "double logarithmic behaviour"

$$xg(x, Q^2) \sim \exp \left(2\sqrt{\xi(Q^2) \ln\left(\frac{1}{x}\right)} \right) \quad (16)$$

where the evolution length $\xi(Q^2)$ is defined as below:

$$\xi(Q^2) = \int_{\mu_0^2}^{Q^2} \frac{dq^2}{q^2} \bar{\alpha}_s(q^2) \sim \log \left(\frac{\log(\frac{Q^2}{\Lambda^2})}{\log(\frac{\mu_0^2}{\Lambda^2})} \right) \quad (17)$$

For very small values of the scale μ_0^2 the evolution length $\xi(Q^2)$ can become large for moderate and large values of Q^2 and the "double logarithmic" behaviour (16) is within the limited region of x , similar to that corresponding to the power like increase of the type $x^{-\lambda}$, $\lambda \approx 0.3$. This explains similarity between the theoretical curves presented in Fig.2.

4. Small x behaviour of the nonsinglet unpolarized and polarized structure functions

The discussion presented in the previous Section concerned the small x behaviour of the singlet structure function which was driven by the gluon through the $g \rightarrow q\bar{q}$ transition. The increase of the gluon distribution in the small x limit implies similar increase of the structure function $F_2(x, Q^2)$. It turns out to be stronger than the increase that would follow from the "soft" pomeron exchange with its relatively low intercept $\alpha_{soft} \approx 1.08$.

The gluons of course decouple from the non-singlet channel and the mechanism of generating the small x behaviour in this case is different.

The simple Regge pole exchange model predicts in this case that

$$F_2^{NS}(x, Q^2) = F_2^p(x, Q^2) - F_2^n(x, Q^2) \sim x^{1-\alpha_{A_2}(0)} \quad (18)$$

where $\alpha_{A_2}(0)$ is the intercept of the A_2 Regge trajectory. For $\alpha_{A_2}(0) \approx 1/2$ this behaviour is stable against the leading order QCD evolution. This follows from the fact that the leading singularity of the moment $\gamma_{qq}(\omega)$ of the splitting function $P_{qq}(z)$:

$$\gamma(\omega) = \int_0^1 \frac{dz}{z} z^\omega P_{qq}(z) \quad (19)$$

is located at $\omega = 0$ and so the (nonperturbative) A_2 Regge pole at $\omega = \alpha_{A_2}(0) \approx 1/2$ remains the leading singularity controlling the small x behaviour of the non-singlet structure function.

The novel feature of the non-singlet channel is the appearance of the **double** logarithmic terms i.e. powers of $\alpha_s \ln^2(1/x)$ at each order of the perturbative expansion. These double logarithmic terms are generated by the ladder diagrams with quark (anti-quark) exchange along the chain. The ladder diagrams can acquire corrections from the "bremsstrahlung" contributions [13, 15] which do not vanish for the polarized structure function $g_1^{NS}(x, Q^2)$ [15].

In the approximation when the leading double logarithmic terms are generated by ladder diagrams illustrated in Fig. 3 the unintegrated non-singlet quark distribution $f_q^{NS}(x, k_t^2)$ ($q^{NS} = u + \bar{u} - d - \bar{d}$) satisfies the following integral equation :

$$f_q^{NS}(x, Q_t^2) = f_{q0}^{NS}(x, Q_t^2) + \tilde{\alpha}_s \int_x^1 \frac{dz}{z} \int_{Q_0^2}^{\frac{Q_t^2}{z}} \frac{dQ_t'^2}{Q_t'^2} f_q^{NS}\left(\frac{x}{z}, Q_t'^2\right) \quad (20)$$

where

$$\tilde{\alpha}_s = \frac{2}{3\pi} \alpha_s \quad (21)$$

and Q_0^2 is the infrared cut-off parameter. The unintegrated distribution $f_q^{NS}(x, Q_t^2)$ is, as usual, related in the following way to the scale dependent (nonsinglet) quark distribution $q^{NS}(x, Q^2)$:

$$q^{NS}(x, Q^2) = \int^{Q^2} \frac{dQ_t^2}{Q_t^2} f_q^{NS}(x, Q_t^2). \quad (22)$$

The upper limit Q_t^2/z in the integral equation (20) follows from the requirement that the virtuality of the quark at the end of the chain is dominated by Q_t^2 . A possible non-perturbative A_2 reggeon contribution has to be introduced in the driving tem i.e.

$$f_{q0}^{NS}(x, Q_t^2) \sim x^{-\alpha_{A_2}(0)} \quad (23)$$

at small x .

Equation (20) implies the following equation for the moment function $\bar{f}_q^{NS}(\omega, Q_t^2)$

$$\bar{f}_q^{NS}(\omega, Q_t^2) = \bar{f}_{q0}^{NS}(\omega, Q_t^2) + \frac{\tilde{\alpha}_s}{\omega} \left[\int_{Q_0^2}^{Q_t^2} \frac{dQ_t'^2}{Q_t'^2} \bar{f}_q^{NS}(\omega, Q_t'^2) + \int_{Q_t^2}^{\infty} \frac{dQ_t'^2}{Q_t'^2} \left(\frac{Q_t^2}{Q_t'^2} \right)^\omega \bar{f}_q^{NS}(\omega, Q_t'^2) \right] \quad (24)$$

Equation (24) follows from (20) after taking into account the following relation:

$$\int_0^1 \frac{dz}{z} z^\omega \Theta \left(\frac{Q_t^2}{Q_t'^2} - z \right) = \frac{1}{\omega} \left[\Theta(Q_t^2 - Q_t'^2) + \left(\frac{Q_t^2}{Q_t'^2} \right)^\omega \Theta(Q_t'^2 - Q_t^2) \right]. \quad (25)$$

For fixed coupling $\tilde{\alpha}_s$ equation (24) can be solved analytically. Assuming for simplicity that the inhomogeneous term is independent of Q_t^2 (i.e. that $\bar{f}_{q0}^{NS}(\omega, Q_t^2) = C(\omega)$) we get the following solution of eq.(24):

$$\bar{f}_q^{NS}(\omega, Q_t^2) = C(\omega) R(\tilde{\alpha}_s, \omega) \left(\frac{Q_t^2}{Q_0^2} \right)^{\gamma^-(\tilde{\alpha}_s, \omega)} \quad (26)$$

where

$$\gamma^-(\tilde{\alpha}_s, \omega) = \frac{\omega - \sqrt{\omega^2 - 4\tilde{\alpha}_s}}{2} \quad (27)$$

and

$$R(\tilde{\alpha}_s, \omega) = \frac{\omega \gamma^-(\tilde{\alpha}_s, \omega)}{\tilde{\alpha}_s}. \quad (28)$$

Equation (27) defines the anomalous dimension of the moment of the non-singlet quark distribution in which the double logarithmic $\ln(1/x)$ terms i.e. the powers of $\frac{\alpha_s}{\omega^2}$ have been resummed to all orders. It can be seen from (27) that this anomalous dimension has a (square root) branch point singularity at $\omega = \bar{\omega}$

$$\bar{\omega} = 2\sqrt{\tilde{\alpha}_s} \quad (29)$$

This singularity will of course be also present in the moment function $\bar{f}_q^{NS}(\omega, Q_t^2)$ itself. It should be noted that in contrast to the BFKL singularity whose position above unity was proportional to α_s , $\bar{\omega}$ is proportional to $\sqrt{\alpha_s}$ - this being the straightforward consequence of the fact that equation (24) sums double logarithmic terms $(\frac{\alpha_s}{\omega^2})^n$. This singularity gives the following contribution to the non-singlet quark distribution $f_q^{NS}(x, Q_t^2)$ at small x :

$$f_q^{NS}(x, Q_t^2) \sim \frac{x^{-\bar{\omega}}}{\ln^{3/2}(1/x)} \quad (30)$$

For small values of the QCD coupling this contribution remains non - leading in comparison to the contribution of the A_2 Regge pole.

As has been mentioned above the corresponding integral equation which resums the double logarithmic terms in the spin dependent quark distributions is more complicated

than the simple ladder equation (20) due to non-vanishing contributions coming from bremsstrahlung diagrams. It may however be shown that, at least as far as the non-singlet structure function is concerned, these contributions give only relatively small correction to $\bar{\omega}$. In what follows we shall therefore limit ourselves to the simple ladder equation (20) assuming that it will describe the spin dependent parton densities as well. The inhomogeneous term will now however be different and will contain the A_1 reggeon contribution. We will limit ourselves to the non-singlet structure function $g_1^{NS}(x, Q^2) = g_1^p(x, Q^2) - g_1^n(x, Q^2) = \Delta q^{NS}/3$ where

$$\Delta q^{NS}(x, Q^2) = \Delta u(x, Q^2) + \bar{\Delta}u(x, Q^2) - \Delta d(x, Q^2) - \bar{\Delta}d(x, Q^2) \quad (31)$$

where $\Delta u, \Delta d$ and $\bar{\Delta}u, \bar{\Delta}d$ denote the corresponding spin dependent quark (antiquark) distributions. We will present an estimate of the effective slope of the non-singlet distributions after numerically solving equation (20) taking into account the asymptotic freedom corrections i.e. allowing the coupling constant α_s to run.

The main interest in applying the QCD evolution equations to study the spin structure function is that the naive Regge pole expectations based on the exchange of low-lying Regge trajectories become unstable against the QCD perturbative "corrections". The relevant reggeon which contributes to $g_1^{NS}(x, Q^2)$ is the A_1 exchange which is expected to have a very low intercept $\alpha_{A_1}(0) \leq 0$. The perturbative singularity generated by the double logarithmic $\ln(1/x)$ resummation can therefore become much more important than in the case of the unpolarized case when it is hidden behind leading A_2 exchange contribution. Even if we restrict ourselves to the leading order QCD evolution [24, 25] then the non-singular $x^{-\alpha_{A_1}(0)}$ behaviour (with $\alpha_{A_1}(0) \leq 0$) becomes unstable as well and the polarized quark densities acquire singular behaviour:

$$\Delta q^{NS}(x, Q^2) \sim \exp(2\sqrt{\xi^{NS}(Q^2)\ln(1/x)}) \quad (32)$$

where

$$\xi^{NS}(Q^2) = \int^{Q^2} \frac{dq^2}{q^2} \tilde{\alpha}_s(q^2) \quad (33)$$

This follows from the fact that $\Delta P_{qq}(z) = P_{qq}(z)$ where $P_{qq}(z)$ and $\Delta P_{qq}(z)$ are the splitting functions describing the evolution of spin independent and spin dependent quark distributions respectively and from the fact that $P_{qq}(z) \rightarrow \text{const}$ as $z \rightarrow 0$.

The introduction of the running coupling effects in equation (24) turns the branch point singularity into the series of poles which accumulate at $\omega = 0$. If one makes the substitution $\tilde{\alpha}_s \rightarrow \tilde{\alpha}_s(Q_t^2)$ then the corresponding equation for the moment can still be solved analytically by reducing it to Kummer's differential equation with the boundary conditions fixed by the requirement that the solution should match the perturbative expansion of the original integral equation [12]. It has however been argued that the theoretically more justified introduction of the running coupling is through the substitution $\tilde{\alpha}_s \rightarrow \tilde{\alpha}_s(Q_t^2/z)$ under the integrand on the rhs. of eq. (20) [14]. We perform a numerical analysis with both prescriptions and estimate the effective slope controlling the small x behaviour of the solution. The two prescriptions of introducing the running coupling effects into the double $\ln(1/x)$ resummation lead to the following integral equation(s) for $\Delta f_q^{NS}(x, Q_t^2)$

$$\Delta f_q^{NS}(x, Q_t^2) = \Delta f_{q0}^{NS}(x, Q_t^2) + \tilde{\alpha}_s(Q_t^2) \int_x^1 \frac{dz}{z} \int_{Q_0^2}^{\frac{Q_t^2}{z}} \frac{dQ_t'^2}{Q_t'^2} \Delta f_q^{NS}\left(\frac{x}{z}, Q_t'^2\right) \quad (34)$$

or

$$\Delta f_q^{NS}(x, Q_t^2) = \Delta f_{q0}^{NS}(x, Q_t^2) + \int_x^1 \frac{dz}{z} \tilde{\alpha}_s(Q_t^2/z) \int_{Q_0^2}^{Q_t^2} \frac{dQ_t'^2}{Q_t'^2} \Delta f_q^{NS}\left(\frac{x}{z}, Q_t'^2\right). \quad (35)$$

We solve these equations numerically, suitably adapting the method developed in [30]. We assume for simplicity that the inhomogeneous term $\Delta f_{q0}^{NS}(x, Q_t^2)$ is independent of both x and of Q_t^2 . The flat x dependence of the inhomogeneous term corresponds to the assumption that $\alpha_{A_1}(0) = 0$. We assume the LO parametrization of the running coupling with four flavours and set $\Lambda = 0.2 \text{ GeV}$. The cut-off parameter Q_0^2 was set equal to $Q_0^2 = 1 \text{ GeV}^2$. In Fig.4 we show the effective slope $\lambda(x, Q_t^2)$ for $Q_t^2 = 10 \text{ GeV}^2$,

$$\lambda(x, Q_t^2) = \frac{d \ln \Delta f_q^{NS}(x, Q_t^2)}{d \ln(1/x)} \quad (36)$$

for the solutions of equation (34) and of equation (35). We also show the effective slope corresponding to the approximation of retaining only the first integral on the right hand side of eq. (34). In this approximation one sums the single logarithmic $\ln(1/x)$ terms accompanied by the leading powers of $\xi^{NS}(Q_t^2)$. The small x behaviour is then asymptotically given by eq.(33). We have also solved eq.(35) assuming that the driving term is given by the A_2 reggeon contribution (see eq.(23)). The resulting slope of the solution is also shown in Fig. 4. It can be seen that the second prescription (i.e $\alpha_s \rightarrow \alpha_s(Q_t^2/z)$) for introducing the running coupling effects makes the effective slope smaller than in the case when one makes the substitution $\alpha_s \rightarrow \alpha_s(Q_t^2)$. The perturbative Regge singularities are not very important for the unpolarized structure functions and the (input) $x^{-1/2}$ behaviour is not altered substantially by the perturbative Regge singularity. The double logarithmic resummation is however very important for generating the singular small x behaviour of the polarized structure functions. The results of our estimate suggest that a reasonable extrapolation of the (non-singlet) polarized quark densities would be to assume an $x^{-\lambda}$ behaviour with $\lambda \approx 0.2$ ³. Similar (or more singular) extrapolations of the spin-dependent quark distributions towards the small x region have been assumed in several recent parametrizations of parton densities [26, 27, 28, 29].

5. Summary and conclusions

In this paper we have briefly summarized the theoretical QCD expectations concerning the small x behaviour of the deep inelastic scattering structure functions in both unpolarized and polarized deep inelastic scattering. In the latter case we have for simplicity focussed on the non-singlet structure functions which, at small x , can be (approximately) described by the ladder diagrams with the quark (antiquark) exchange. We have solved the corresponding integral equation taking into account asymptotic freedom effects and estimated the effective slope controlling the small x behaviour of the non-singlet structure function. The perturbative QCD effects become significantly amplified for the singlet spin structure function due to the mixing with the gluons. The simple ladder equation may not however be applicable for an accurate description of the double logarithmic terms in the polarized gluon distribution ΔG .

³ The effective slope λ turns out to depend weakly upon the infrared cut-off parameter Q_0^2 . If we set $Q_0^2 = \Lambda^2$ then $\lambda \rightarrow \frac{8}{(33-2N_f)} = 0.32$. I thank Misha Ryskin for pointing out this fact to me.

Acknowledgments

I thank Alan Martin and Peter Sutton for most enjoyable research collaboration on the problems presented in this paper. I thank them as well as Jochen Bartels, Misha Ryskin and Andreas Schäfer for illuminating discussions. I am grateful to Grey College and Physics Department of the University of Durham for their warm hospitality. This research has been supported in part by the Polish State Committee for Scientific Research grant 2 P302 062 04 and the EU under contracts n0. CHRX-CT92-0004/CT93-357.

References

- [1] B. Badelek et al., Rev. Mod. Phys. **64** (1992) 927.
- [2] A.D. Martin, Acta. Phys. Polon, **B25** (1994) 265.
- [3] J. Kwieciński, Nucl. Phys. B (Proc. Suppl.) **39 B,C** (1995) 58.
- [4] E.A. Kuraev, L.N.Lipatov and V.Fadin, Zh. Eksp. Teor. Fiz. **72** (1977) 373 (Sov. Phys. JETP **45** (1977) 199); Ya. Ya. Balitzkij and L.N. Lipatov, Yad. Fiz. **28** (1978) 1597 (Sov. J. Nucl. Phys. **28** (1978) 822); L.N. Lipatov, in "Perturbative QCD", edited by A.H. Mueller, (World Scientific, Singapore, 1989), p. 441; J.B. Bronzan and R.L. Sugar, Phys. Rev. **D17** (1978) 585; T. Jaroszewicz, Acta. Phys. Polon. **B11** (1980) 965.
- [5] A.J. Askew et al., Phys. Rev. **D47** (1993)3775; Phys. Rev. **D49** (1994) 4402.
- [6] H1 collaboration: A. de Roeck et al., preliminary measurements to be published in the Proc of the Workshop on DIS and QCD, Paris, 1995, DESY preprint 95 - 152.
- [7] ZEUS collaboration: B. Foster, to be published in the Proc. of the Workshop on DIS and QCD, Paris, 1995, DESY preprint 95-193.
- [8] A. Donnachie and P.V. Landshoff, Phys. Lett. **B296** (1992) 257.
- [9] P.D.B. Collins, "An Introduction to Regge Theory and High Energy Physics", Cambridge University Press, Cambridge, 1977.
- [10] B.L. Ioffe, V.A. Khoze and L.N. Lipatov, "Hard Processes", North Holland, Amsterdam-Oxford-NewYork-Tokyo, 1984.
- [11] V.G. Gorshkov et al., Yad. Fiz. **6** (1967) 129 (Sov. J. Nucl. Phys. **6** (1968) 95); L.N. Lipatov, Zh. Eksp. Teor. Fiz. **54** (1968) 1520 (Sov. Phys. JETP **27** (1968) 814).
- [12] J. Kwieciński, Phys. Rev. **D26** (1982) 3293.
- [13] R. Kirschner and L.N. Lipatov, Nucl. Phys. **B213** (1983) 122.
- [14] B.I. Ermolaev, S.I. Manayenkov and M.G. Ryskin, DESY preprint 95-017.
- [15] J. Bartels, B.I. Ermolaev and M.G. Ryskin, DESY preprint 95 - 124.

- [16] M. Ciafaloni, Nucl. Phys. **B296** (1988) 49.
- [17] S. Catani, F. Fiorani and G. Marchesini, Phys. Lett. **B234** (1990) 339; Nucl. Phys. **B336** (1990) 18; G. Marchesini, in Proceedings of the Workshop "QCD at 200 TeV", Erice, Italy, 1990, edited by L. Cifarelli and Yu. L. Dokshitzer (Plenum Press, New York, 1992), p. 183; G. Marchesini, Nucl. Phys. **B445** (1995) 49.
- [18] J. Kwieciński, A.D. Martin, P.J. Sutton, Phys. Rev. **D52** (1995) 1445.
- [19] A.D. Martin, J. Kwieciński and P.J. Sutton, Nucl. Phys. B (Proc. Suppl.) **A29** (1992) 67
- [20] S. Catani, M. Ciafaloni and F. Hautmann, Phys. Lett. **B242** (1990) 97; Nucl. Phys. **B366** (1991) 657; J.C. Collins and R.K. Ellis, Nucl. Phys. **B 360** (1991) 3; S. Catani and F. Hautmann, Nucl. Phys. **B427** (1994); M. Ciafaloni, Phys. Lett. **356** (1995) 74.
- [21] J. Kwieciński, A.D. Martin and P.J. Sutton, Durham preprint DTP/95/94.
- [22] A.D. Martin, R.G. Roberts and W.J. Stirling, Phys. Rev. **D50** (1994) 6734; Phys. Lett. **354** (1995) 155.
- [23] M. Glück, E. Reya and A. Vogt, Z.Phys. **C67** (1995) 433.
- [24] M.A. Ahmed and G.G. Ross, Phys. Lett. **B56** (1975) 385; Nucl. Phys. **B11** (1976) 298; G. Altarelli and G. Parisi, Nucl. Phys. **B126** (1977) 298.
- [25] R.D. Ball, S. Forte and G. Ridolfi, Nucl. Phys. **B444** (1995) 287.
- [26] C. Bourrely and J. Soffer, Phys. Rev. **D51** (1995) 2108; Nucl. Phys. **B445** (1995) 341; Marseille preprint CPT-95/P.3224.
- [27] M. Glück, E. Reya and W. Vogelsang, Phys. Lett. **B359** (1995) 201.
- [28] T. Gehrmann and W.J. Stirling, Durham preprint DTP/95/62.
- [29] J. Blümlein and A. Vogt, DESY preprint 95-175.
- [30] J. Kwieciński, Z. Phys. **C29** (1985) 561.

Figure captions

1. Diagrammatic representation of the k_t factorization formula (13).
2. A comparison of the HERA measurements of F_2 [6, 7] with the predictions based on the k_t factorization formula (13) using for the unintegrated gluon distributions f the solutions of the CCFM equation (14) (continuous curve) and of the approximate form of this equation corresponding to setting $\Theta(Q - q)$ in place of $\Theta(Q - qx/x')$ and $\Delta_R = 1$ (dotted curve). We also show the values of F_2 obtained from collinear factorization using the MRS(A') [22] and GRV [23] partons (the figure is taken from ref. [21]).
3. The ladder diagram with quark (antiquark) exchange along the chain.

4. The effective slope $\lambda(x, Q_t^2)$ defined by the formula (36) of the solutions of the equations (34) (dashed curve) and (35) (solid curve). The dashed-dotted curve corresponds to the approximation of eq. (34) in which only the first integral on right hand side is retained. The dotted curve represents the slope of the solution of eq. (35) in which the inhomogeneous term is set proportional to $x^{-1/2}$. The slopes are plotted as functions of x for fixed $Q_t^2 = 10GeV^2$.

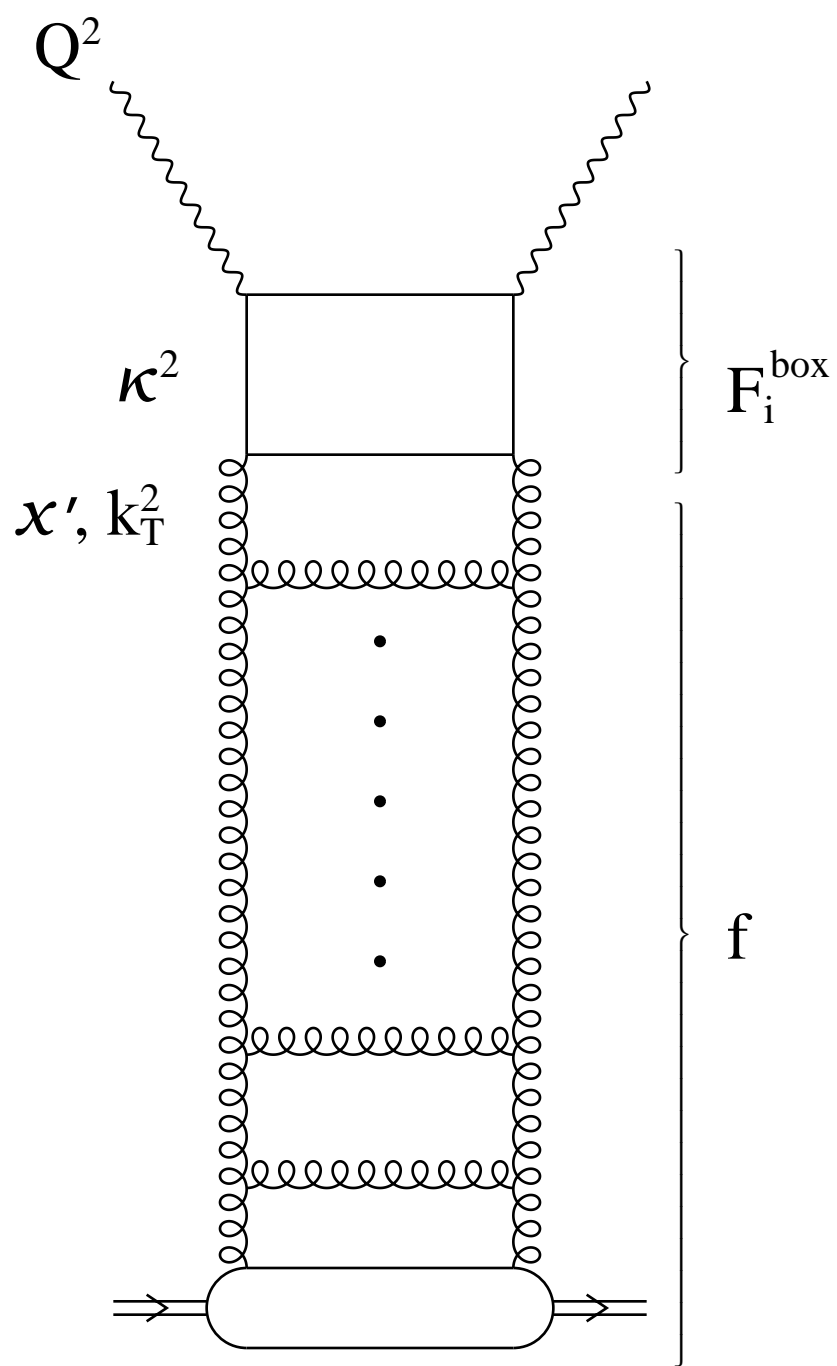


Fig. 1

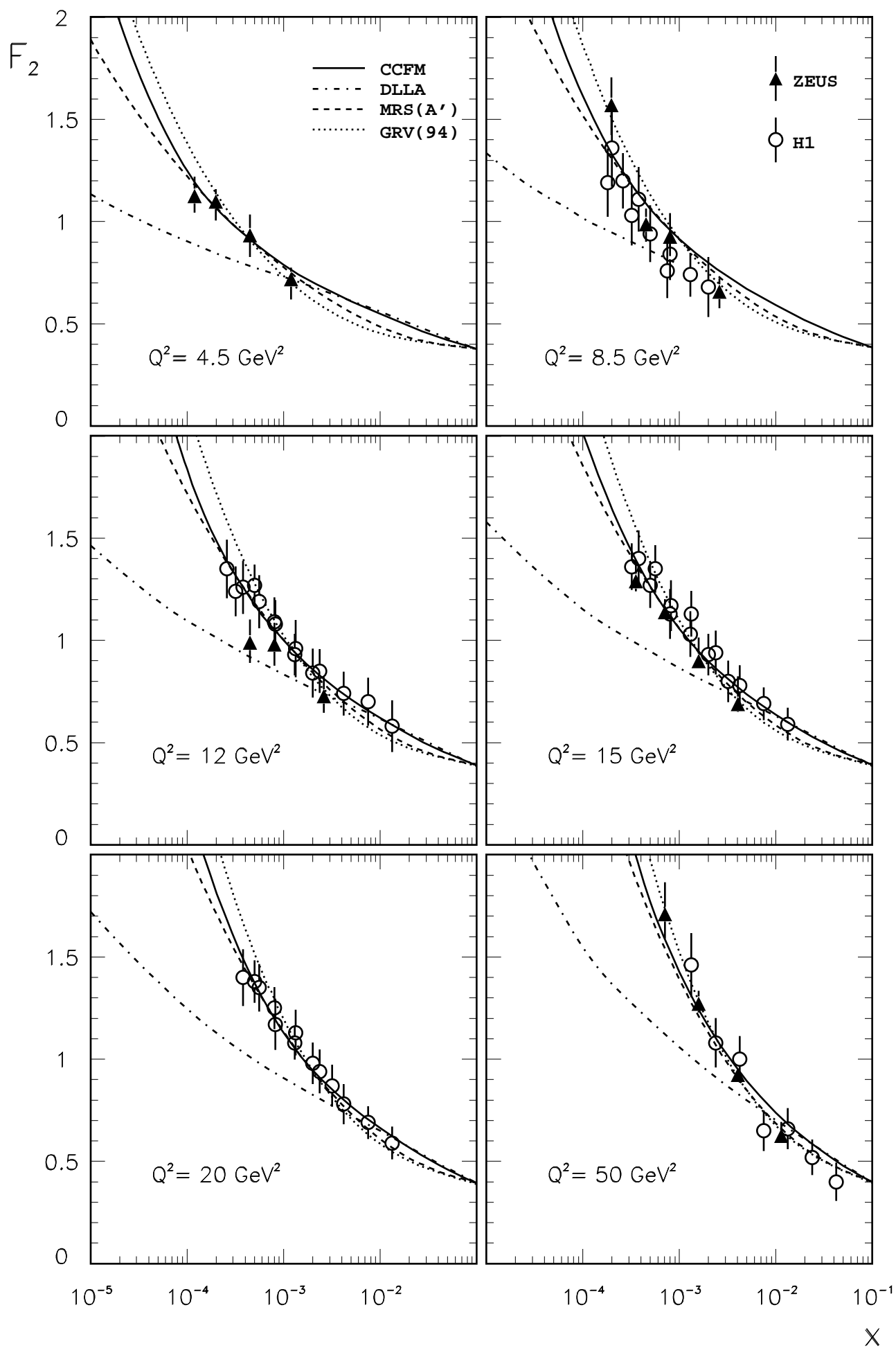
Fig.2

Fig.4

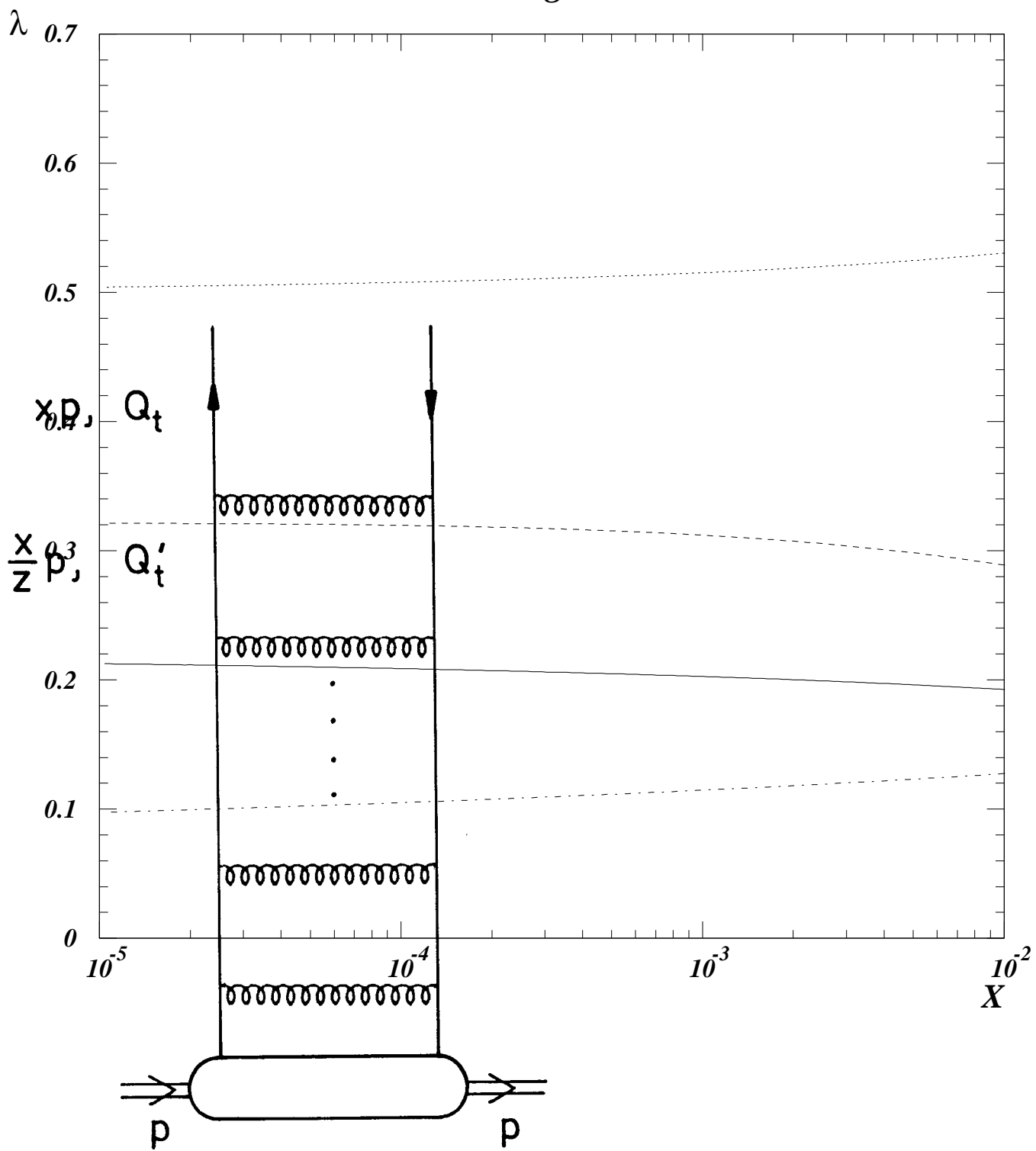


Fig. 3